Computers and Chemical Engineering 181 (2024) 108545

Contents lists available at ScienceDirect

Computers and Chemical Engineering

journal homepage: www.elsevier.com/locate/compchemeng

Technoeconomic evaluation of post-combustion carbon capture technologies on-board a medium range tanker

Preethi Sridhar, Anikesh Kumar, Sanjith Manivannan, Shamsuzzaman Farooq *, Iftekhar A. Karimi *

Department of Chemical and Biomolecular Engineering, National University of Singapore, 4 Engineering Drive 4, 117585, Singapore

ARTICLE INFO

Keywords:
Carbon capture
GHG emissions
Maritime capture
Amine-based absorption
Cryogenic separation

ABSTRACT

The international maritime organization has recently set targets and timelines for reducing global greenhouse gas emissions from the maritime industry, which currently stand at 1.1 Gt/year and make 3 % of the global emissions. Reducing emissions by increasing engine efficacy is the immediate target, but there is a limit to how much this path can achieve. Onboard post-combustion carbon capture and concentration in large marine vessels is emerging as an interim approach to reduce maritime emissions until large-scale deployment of low/zero emission fuels become viable. In this paper, we evaluate three carbon capture technologies (chemical absorption using either aqueous MEA or aqueous NH_3 as the solvent, cryogenic separation, and membrane separation) for a medium-range tanker for two fuels, namely heavy fuel oil and liquefied natural gas. The capture cost per tonne of CO_2 (recovery>90 %, purity>95 %) was considered as the assessment criterion, with simultaneous evaluation of other aspects such as energy and space demands. The simulations were carried out using MATLAB and ASPEN V12. For rate-based models, the adjustable parameters for the model were tuned using pilot plant data. Additionally, options for hot and cold energy integration were also assessed and implemented. Based on the reference ship conditions and assessment criteria, the simulation studies show that amine-based absorption is the best prospect for on-board capture by a clear margin.

1. Introduction

The maritime industry contributes about 3 % (1.1 Gt/year) of global greenhouse gas (GHG) emissions (IMO, 2015), which is receiving attention. The annual GHG emissions (over 98 % contributed by CO_2 emissions) from ships increased by 9.6 % (977 to 1076 million tonnes) from 2012 to 2018, thus making the maritime share of global anthropogenic CO_2 emissions rise from 2.76 % to 2.89 % in the same time span (IMO, 2021b). In line with the worldwide efforts to reduce GHG emissions, the international maritime organization (IMO) has introduced annexures/guidelines on reducing maritime emissions as shown in Fig. 1 (IMO, 2021a), with the eventual target of 50 % reduction in GHG emissions by 2050 taking 2008 as the benchmark year.

Conventionally, heavy fuel oils (HFOs) have been predominantly used as marine fuel. However, their high emissions have led to recent efforts on improving ship's engine efficiency and gradually switching to low carbon and low sulphur fuels like marine gas oil (MGO), and biofuels. Additionally, new ships are being built to use liquified natural gas (LNG) as the fuel, which has negligible SOx emission and can reduce CO_2 emissions by 20–30 % (Awoyomi et al., 2020). Another mitigation strategy that has been considered by IMO is that of imposing carbon taxes. However, the tax policy needs to be straightforward and easy to implement, and has to be developed in phases so as to minimize disruptions. Moreover, it has to encompass the interests of all its stakeholders. For example, it should be mindful of the concerns of small-island developing states and adopt prudent mechanisms of compensation for them (Parry et al., 2018). Even if the aforementioned issues are addressed over time, imposing carbon tax alone cannot achieve the reduction targets. To this end, zero emission fuels like hydrogen and ammonia hold the ultimate solution. However, their wide deployment will take time. In the interim, on-board CO_2 capture and concentration (CCC) is receiving attention as an essential transition strategy to reduce emissions from ships until zero emission technologies become widely available.

Technologies investigated in the literature for onboard CCC are largely focused on absorption-based separation. Luo and Wang (2017)

* Corresponding authors.
E-mail addresses: chesf@nus.edu.sg (S. Farooq), cheiak@nus.edu.sg (I.A. Karimi).

https://doi.org/10.1016/j.compchemeng.2023.108545
Received 22 April 2023; Received in revised form 21 November 2023; Accepted 2 December 2023
Available online 3 December 2023

carried out a study on monoethanolamine (MEA) for diesel fuelled (cargo) ships and found that the waste heat was sufficient for 73 % capture at 77.5 €/tCO_2. 90 % capture requires an extra turbine to supply the additional energy and increases the capture cost to 163 €/tCO_2. Feenstra et al. (2019) investigated MEA and piperazine (PZ) for diesel and LNG ships. They concluded that the thermal energy extracted from the flue gas is sufficient to supply the reboiler duty for 90 % capture. However, Einbu et al. (2022) contradict this finding, claiming that the excess flue gas heat is sufficient only for 50 % capture. Additionally, Feenstra et al. (2019) showed PZ to be a more cost-effective solvent with 98 €/tCO_2 as the least cost; however, the literature deems it unfit for use, as it has low biodegradability (Eide-Haugmo et al., 2012; Ros et al., 2022).

NH_3 has emerged as another promising solvent owing to its low heat duty for regeneration and the potential for capturing CO_2, SO_2, and NOx simultaneously (Niu et al., 2012; Yeh et al., 2005). However, high concentrations of NH_3 are ecotoxic and hence undesirable (Eide--Haugmo et al., 2012). Additionally, due to its innately high volatile nature, solvent loss is a critical challenge (Zhang and Guo, 2013). Taking cognizance of these constraints, Awoyomi et al. (2020) considered aqueous ammonia solvent for LNG fuelled ships. To keep within the NH_3 discharge limit, they suggested recovering NH_3 by using a wash column. The largest waste treatment facilities in ships can handle water up to 100 kl/day (Wärtsilä, 2019a), but even that will be insufficient to handle the demand incurred by the wash column effluent. To account for this, additional cost for plant upsizing should be incorporated in the overall capture cost. Alternately, the cost for an abatement section for the solvent should be included (See Section 3.2).

Although the literature studies for maritime capture are largely focused on absorption-based separation, most of these works for on-board capture have not discussed the details of the rate-based mass transfer model used in simulations. This comprises information on different models and correlations used, as well as tuning of the model parameters to calibrate the model predictions with experimental/pilot plant data. Awoyomi et al. (2019) discuss the selection of suitable kinetic data and mass transfer correlations for NH_3 solvent; however, they exclude parameter tuning for the simulation studies. Amirkhosrow et al. (2021) have carried out a similar study for MEA solvent; however their studies fall outside of the CO2 concentrations pertinent to maritime studies. Additionally, tuning of some of the essential parameters is not discussed.

Oh et al. (2022) have studied membrane separation for LNG fuelled ships for binary (CO_2, N_2) and ternary (CO_2, N_2, O_2) flue gas systems. The work carries out energy optimization of a two-stage membrane system with provision for recycle together with different refrigeration cycles. However, the work does not carry out costing for the capture system nesessary to compare its commercial viability against other capture designs available in the literature. Additionally, the presence of moisture in flue gas is completely ignored, which diminishes its practical relevance.

Cryogenic separation technologies like distillation, condensation and sublimation have been widely studied for CO_2 capture (Shen et al., 2022). However, to the best of our knowledge, no study for on-board capture using cryogenic separation exists in the literature. For on-board capture, condensation seems to be the most plausible process as distillation requires high cost and is suitable for high concentrations (H. Yang et al., 2008), whereas sublimation has high refrigeration costs and requires solid handling (Song et al., 2019).

Lastly, to the best of our knowledge, despite being a widely studied method for CCC, adsorption has not been investigated for on-board capture in marine vessels. Vacuum Swing Adsorption (VSA) and Temperature Swing Adsorption (TSA), are the commonly investigated two versions of the adsorption technology CCC for coal fired power plants with approximately 15 % CO_2 in the flue gas. Peh et al. (2023) have discussed that cost and plant footprint are the current challenges of these two technologies for their industrial implementation. These predicaments increase manyfold at even lower CO_2 concentration, which is in the range 3–7 % in marine applications. For these reasons, the adsorption technology is not considered for onboard CCC from the flue gas of a marine vessel.

1.1. Scope of work

As discussed above, some limitations of the literature on maritime CCC are as follows:

- Ø Studies on chemical absorption have not discussed the selection of appropriate correlations, models, and parameter tuning for rate-based models using different solvents.
- Ø Awoyomi et al. (2020) investigated ammonia stripping for an LNG run ship; however, they did not consider the cost of upscaling the water treatment plant in the ship to process the NH_3 rich wash water.

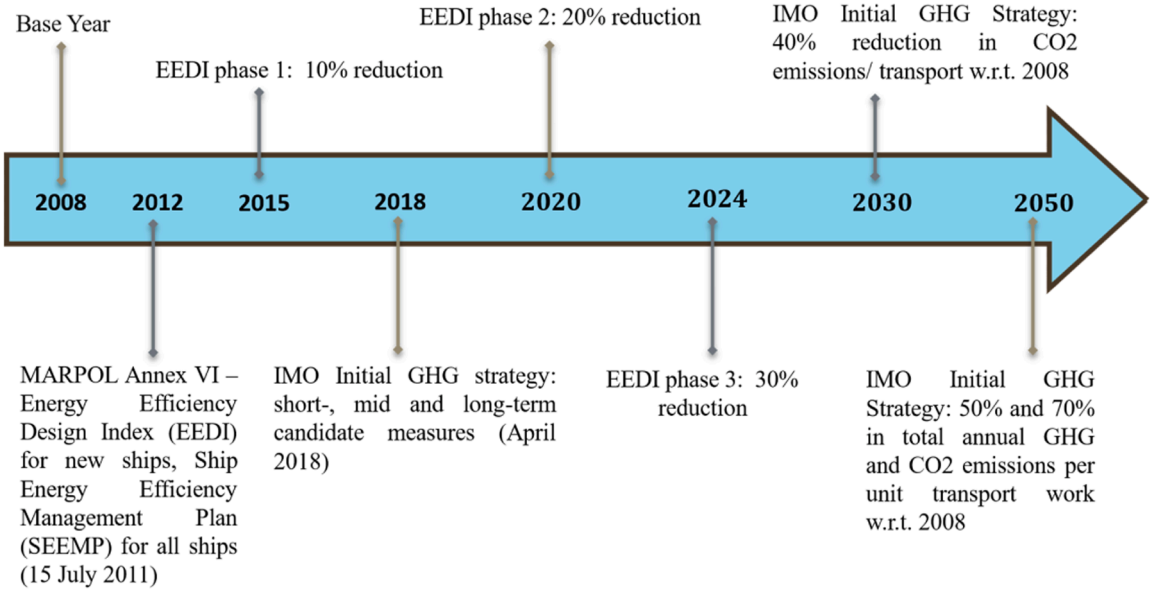

Fig. 1. Timeline for reduction in maritime emissions.

- There is no study on onboard capture using cryogenic separation.
- Oh et al. (2022) studied membrane-based onboard capture; however, they did not calculate the cost of capture.
- Lastly, no work in the literature has made a comparative assessment of different CCC technologies on a single consistent platform for a given ship/flue gas conditions in order to shed light on their respective benefits, challenges, and limitations.

To address these limitations, in this work, a comparative assessment is carried out for absorption with two solvents (MEA and NH_3), cryogenic condensation, and membrane separation technologies including appropriate pre-conditioning of the flue gas and liquefaction of the concentrated CO_2. Fig. 2 is the process schematic showing all three options. It should be noted that cryogenic condensation process is common for all the three routes. It either receives flue gas feed directly without any enrichment or concentrated CO_2 from the absorption or the membrane process for liquefaction. The simulations were carried out using Aspen V12 and MATLAB. Appropriate correlations and parameters for rate-based models for both MEA and NH_3 are also provided along with validation studies using pilot plant data. The total annual cost (TAC) per tonne of CO_2 captured ($/t$CO_2$) is considered as the primary assesment criteria subject to lower bounds of 90 % and 95 % on the recovery and purity of CO_2 respectively. For screening technologies, recovery is defined on the basis of the CO_2 emissions from the original ship engine excluding any extra emissions that may stem from thermal energy/power demand for a given CCC technology. However, for the top ranked technology, we report the effective recovery considering the extra emissions.The costing methodology is covered in Section 5. Other key performance indicators (KPIs) are extra cold and hot energy requirements above what is available in the ship, and cargo weight and volume losses incurred by the capture unit, and these are dicussed for the best prospective technology.

2. Basis for design and comparison

Vessel type and size are critical in the selection of onboard capture technologies. According to a published report (UNCTAD, 2020), there has been a recent transition towards larger tankers, containers, and bulk vessels to take advantage of the scale and reduce the CO_2 emissions per tonne-mile. Tankers in particular have had 19 % increase in CO_2 emissions from 2011 to 2019, thus making them an important class of vessels to investigate onboard CO_2 capture. Hence, in this work, simulation studies were carried out for capture onboard a medium range (MR) tanker. The vessel is assumed to be on sea for 8 months with a single trip lasting 15 days. The flue gas conditions were chosen corresponding to a 10,035 kW HFO Engine at 75 % MCR (maximum continuous rating) load operating in tropical conditions. Additionally, as mentioned, LNG is gaining traction as a shipping fuel. Hence, flue gas conditions for an LNG engine of equivalent power, taken from Wärtsilä (2019b), are also investigated in the simulation studies. The flue gas conditions for both the fuels are summarized in Table 1.

The rest of the paper is organized as follows. Section 3 contains process descriptions of the potential technologies for CCC. The details of the rate based model for absorption with chemical reaction using MEA and NH_3 solvents as well as model equations for membrane separation are discussed in Section 4. Simulation results and TAC evaluation for all the technologies is discussed in Section 5. Next, the other key performance indicators (KPIs) pertaining to maritime capture, discussed in Section 6, for the most cost-effective technology are dicussed in Section 6. The findings of this work are summarized in Section 7.

Table 1
Flue gas conditions for HFO and LNG run engines.

Specification	HFO	LNG
Main engine	10,035 kW Wärtsilä 9L46DF	9960 kW MAN 6S50ME-C8.5
Exhaust gas flow rate at 75% load (kg/s)	17.4	12.3
Air flow Rate at 75% load (kg/s)	17.1	12.45
Exhaust gas temperature (°C)	256	390
Exhaust gas pressure (Pa g)	3500	3500
CO_2 (mol%)	4.00	2.79
N_2 (mol%)	73.04	75.31
H_2O (mol%)	12.95	6.19
O_2 (mol%)	9.11	14.80
Ar (mol%)	0.86	0.90
SO_2 (mol%)	0.05	0

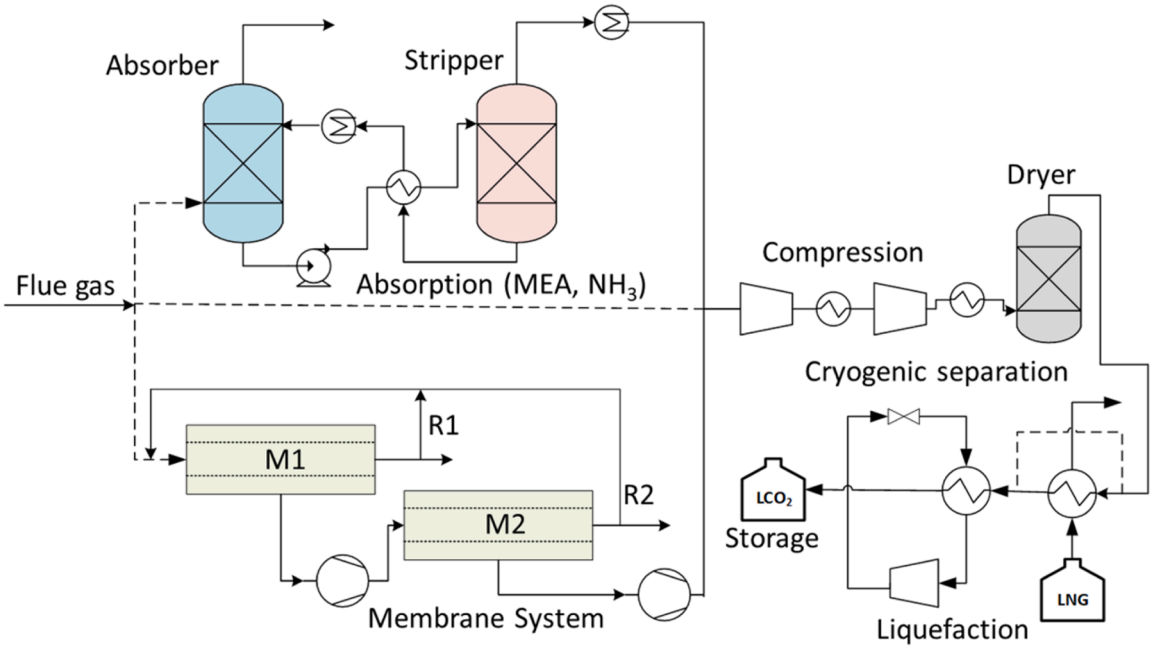

Fig. 2. Prospective technologies for on-board CO_2 capture.

3. Process description

In this section, the major equipment, operating conditions, and energy integration for the different prospective technologies for onboard capture are discussed.

3.1. Absorption with MEA

The absorption-based CCC comprises an absorber, a regenerator, a lean-rich heat exchanger followed by a compression and liquefaction section, as shown in Fig. 3. The exhaust gas is cooled and pressurized to 45 °C and 0.05 barg respectively, before entering the CCC unit, as recommended by Stec et al. (2021). The pressurization is carried out with the aid of a blower and the cooling is done in two stages. In the first stage, waste heat energy (WHR) from the exhaust gas is used to generate low pressure (LP) steam for CO_2 regeneration and the gas is cooled to 140 °C. The rest of the cooling is achieved in the second stage by using cooling water. The cooled exhaust gas is sent to the pre-treatment facility for SOx removal in the case of HFO, but for LNG desulfurization is not required. A 30 wt % aqueous MEA solution is used for CO_2 removal in the absorber, as suggested in the literature (Adu et al., 2020; Stec et al., 2021).

The vapour stream from the regenerator unit comes out at 2 bar and 45 °C and contains ~95 % CO_2 by volume. Liquid CO_2 is the most widely used form of CO_2 storage owing to ease of transport, improved storage capacity and safety conditions (Aspelund et al., 2006). In this work, the storage pressure is fixed at 16 bar (CO_2 dew point: ~−29 °C) and uses two stages of compression with equal pressure ratios. The CO_2 stream is cooled to 45 °C after each compression stage using cooling water and the water condensed in the process is removed using flash separators. In order to liquefy the compressed gas at 16 bar, it needs to be cooled further. Before cooling it further, the compressed gas is first sent into a dryer to remove the residual moisture in order to prevent formation of hydrates/ice. Drying is assumed to be carried out via adsorption with a silica-based adsorbent. For the HFO case, the cooling is carried out with the aid of a refrigeration cycle; however, in the case of LNG, it may be possible to completely eliminate the refrigeration cycle in some scenarios and in some other scenarios the power demand of the refrigeration cycle can be reduced using LNG cold. In this work, NH_3 has been chosen as the refrigerant due to its wide acceptance in the maritime industry. The liquefied CO_2 is stored in cylindrical storage tanks at 85 % of the maximum capacity. Boil-off gas (BOG) generated from storing CO_2 at cryogenic temperatures is assumed to be 0.03 % and is recycled back to the compressor inlet.

3.2. Absorption with NH_3

The NH_3 based capture process consists of a typical desulphurization column (in case of HFO powered ship), absorber and a regenerator similar to the system in the preceding section. However, to comply with the mandatory NH_3 emission standards under the Environmental Protection and Management (Air Impurities) Regulations (SingaporeStatutesOnline, 2023), an additional abatement section is required (see Fig. 4). NH_3 is removed from the vent gas of the absorber column in the abatement section using a wash column, and the NH_3-rich wash bottom is sent to a regenerator unit. The regenerated NH_3 is recycled back as solvent makeup in the CO_2 absorber column, thereby reducing the solvent makeup requirement. Compared to MEA, NH_3 has a higher CO_2 absorption rate; and hence, requires a lower reagent concentration (Jayaweera et al., 2016). A reagent concentration of 10 wt %, suggested by Awoyomi et al. (2020), is used for simulations. However, the operating temperature suggested in their work (26 °C) leads to an ammonia slip of ~95,000 ppm, which requires a very high-water flowrate in the wash column leading to a very high reboiler duty for NH_3 recovery. To reduce the slip and in turn the regeneration duty in the abatement section, chilled NH_3 at 10 °C is used in this work. The CO_2 from the separation section regenerator unit in this case is received at 6 bar and is compressed to 16 bar. Since, there is a reduction in the required pressure ratio, only one stage of compression is needed.

3.3. Cryogenic condensation

Unlike absorption, cryogenic condensation does not comprise tall columns or pre-processing units for SO_x and NO_x, thus making it very compact and hence an interesting prospect for onboard capture. The cryogenic separation is modelled using Peng Robinson (Notz et al.) EOS. The work reported by W. Yang et al. (2015) has analysed experimental data validation of N_2/CO_2 cryogenic system to be in good agreement with PR model. The exhaust gas from the ship engine is sent into a two-stage compression train with equal pressure ratios to achieve a pressure of 16 bar. The gas is cooled to 45 °C by water coolers at the exit of the compressor units and the condensate is removed using flash separators. The water depleted stream (~100 % moisture removal) post drying unit is sent to the liquefaction section where the components are separated based on difference in their dew points.

In the liquefaction section, the outlet gas stream from the

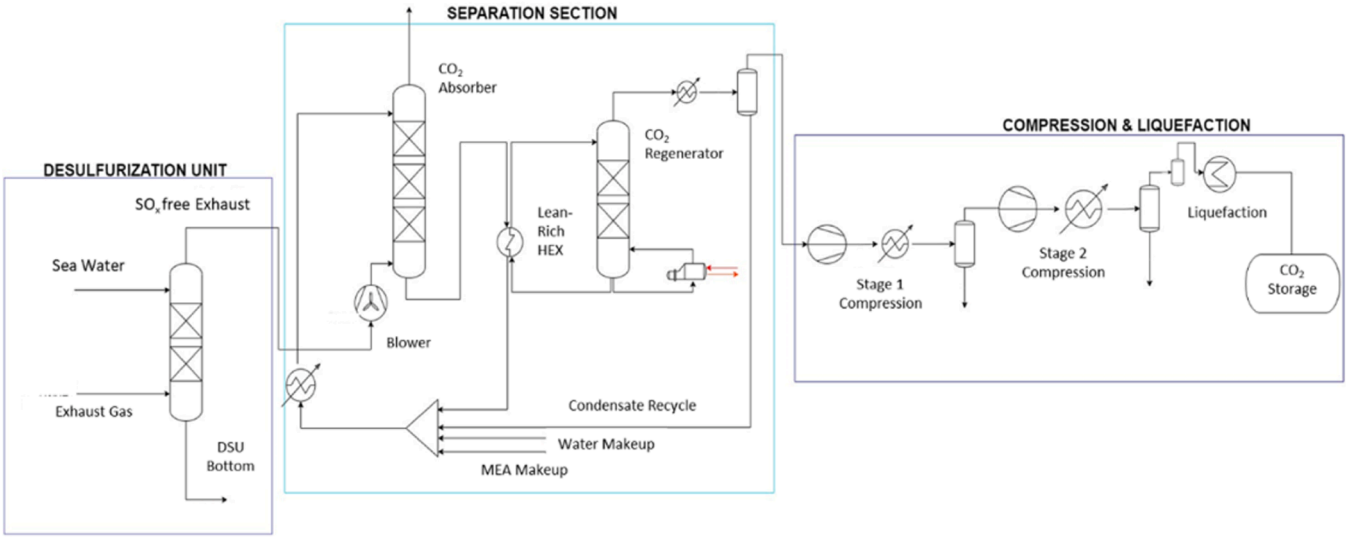

Fig. 3. Process Flow Sheet of MEA based CO_2 capture. (changed).

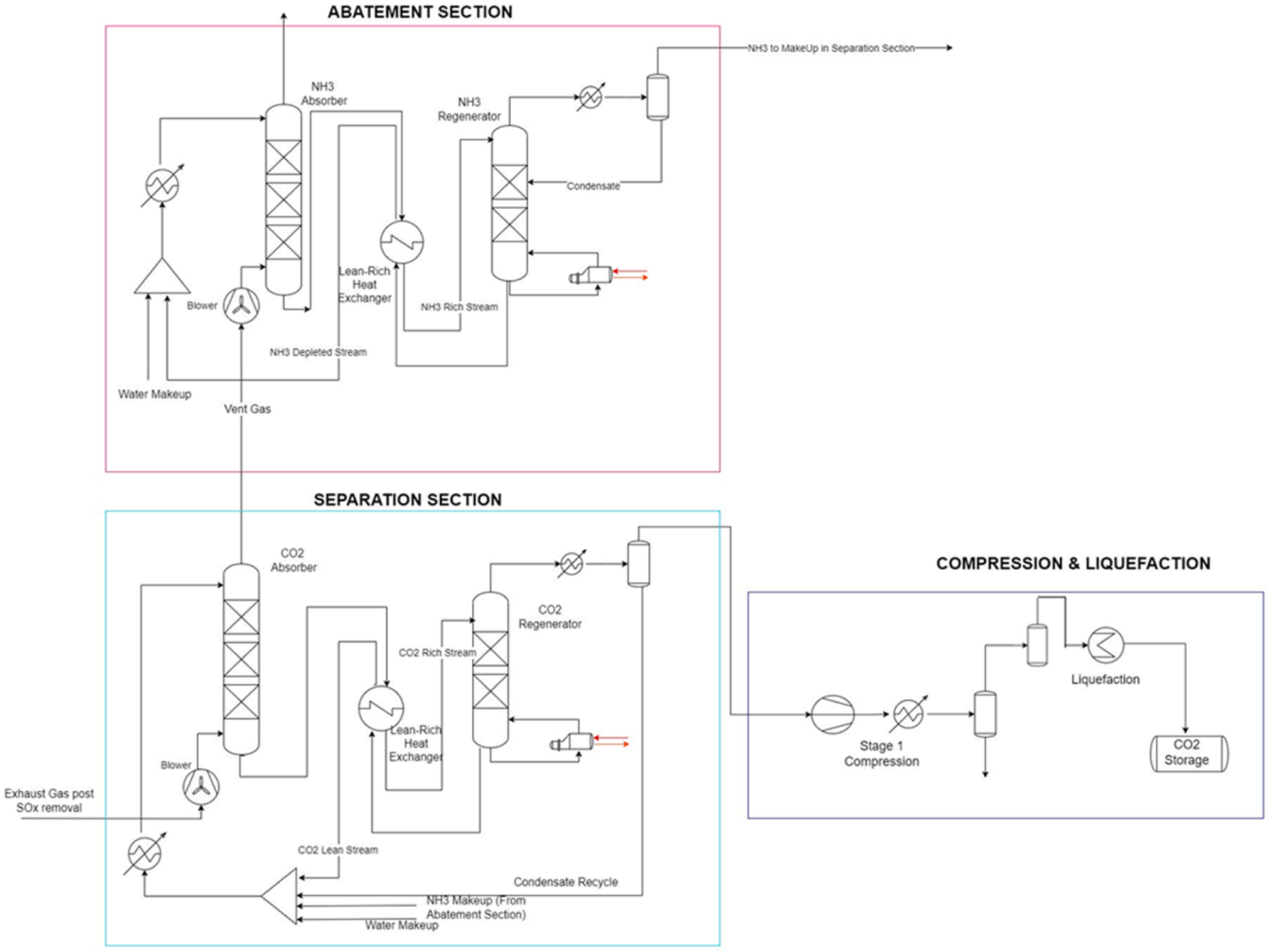

Fig. 4. Process Flow Sheet of NH_3 based CO_2 capture.

compression section is routed through a MSHE (multi-stream heat exchanger) as shown in Fig. 5. The liquefaction unit retrieves cold energy from the N_2 stream from the exhaust gas in the HFO case and from both N_2 and LNG cold energy in the LNG case. However, the cold energy is insufficient for complete condensation of CO_2 in both cases. Hence, a refrigeration unit is required to aid the liquefaction of CO_2.

Natural working fluids (NWFs) (N_2, NH_3, C_3H_6 etc.) are preferred due to the very low global warming potential (GWP). N_2 is selected as the refrigerant due to its lower boiling point (−192 °C) compared to other NWFs necessary to provide requisite cooling for condensation of low concentration CO_2 in this process.

3.4. Membrane separation

In this work, a 2-stage membrane separation unit with the possibility of recycling the raffinate stream from both stages is considered (see Fig. 2) for a 4-component system comprising CO_2, N_2, O_2, and H_2O. For enhancement of the driving force, vacuum on the permeate side is used instead of feed compression as the literature suggests it to be the more cost-efficient method for membrane separation. A complete mixing pattern is used for the membrane model (Geankoplis, 2003). The operation of the membrane is assumed to be isothermal with negligible pressure drop on either side. The mathematical model for the membrane process is discussed in Section 4.

4. Simulation methodology

In this section, details of rate-based models for absorption and model equations for membrane separation are discussed.

4.1. Parameters and correlations for rate-based model

In this work, CCC via absorption with MEA and NH_3 solvents is assessed using an accurate high-fidelity rate-based simulation model. The thermodynamic properties are chosen to be e-NRTL and SRK for liquid and gas side properties for both solvents. The equilibrium and kinetically controlled reaction sets for CO_2 absorption with both solvents are provided in Supporting Information. For an accurate rate-based model in Aspen Plus, appropriate kinetic data, mass and heat transfer correlations, and numerical parameters are paramount. For NH_3, these are readily available from Liu et al. (2015), the literature studies on MEA lack information on the numerical parameters. For MEA, the rate-based model is calibrated in Aspen Plus using experimental data from Notz et al. (2012) which contains 47 different experiments with variations in different parameters like flue gas and solvent conditions (flow, temperature, pressure, composition) resulting in different capture rates for fixed column dimensions. For the purpose of this study, 13 different experiments were chosen (Table S1, see Notz et al. (2012) for more details) that are representative of the flue gas conditions pertinent to maritime studies.

The mass transfer model for absorption in Aspen Plus uses is based on

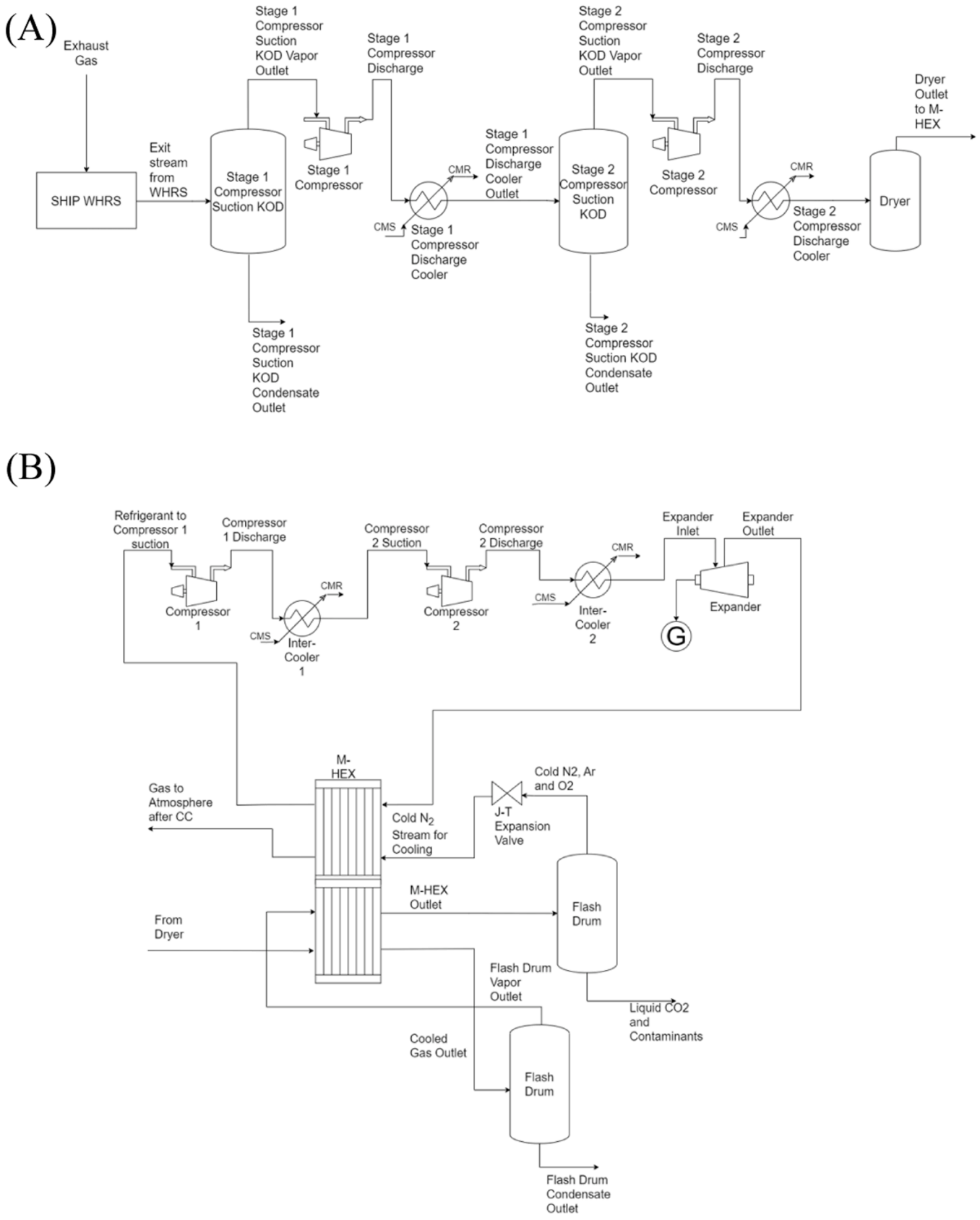

Fig. 5. Process Flow Diagram for Cryogenic Carbon Capture (A): Compression Section (B): Liquefaction Section.

the two-film theory (Lewis and Whitman, 1924). The key model specifications and correlations used in the models for MEA and NH_3 are listed in Table 2. Further details on these models/correlations are provided in the supplementary information.

In addition to the above descriptors, several numerical parameters must be fixed to ensure accurate and stable simulation results without excessive computation time. These are NADP, NFDP, FDR, MCF, and RCF listed and described in Table 3. In order to fix NADP, we observed the changes in column profiles for temperature and CO_2 concentration in the liquid phase for the range of NADP values listed in Table 3. Since, the column profiles do not change much beyond NADP=55, its value was fixed as 55. Next, with other numerical parameters fixed, we varied NFDP to observe the changes in the absolute relative deviation (ARD) in the prediction error of the CO_2 capture efficiency as defined below:

$$ARD(k) = \left| \frac{eff_{ex}(k) - eff_{model}(k)}{eff_{ex}(k)} \right| \times 100 \tag{1}$$

$$eff_{co2} = \frac{CO_{2,in} - CO_{2,out}}{CO_{2,in}} \times 100 \tag{2}$$

where eff_{ex} and eff_{model} are the capture efficiencies measured from the experiment and predicted by the model, and $CO_{2,in}$ and $CO_{2,out}$ are the CO_2 flow rates entering and exiting the absorption column.

It was observed that the ARD does not vary significantly for NFDP>5. Hence, a NFDP value of 5 was chosen for the simulations. Next, FDR along with condition factors (MCF and RCF) was tuned by optimizing the average and standard deviation of ARD (Eq. (3)) across different experiments.

$$AARD = \frac{\sum_{k=1}^{n} ARD(k)}{n}, \; SDARD = \sqrt{\frac{\sum_{k=1}^{n} (ARD(k) - AARD)^2}{n}} \tag{3}$$

The optimal values were found to be $RCF = 0.75$, $MCF = 0.25$, $FDR = 2.5$. Details of the tuning studies have been omitted here for the sake of brevity and can be found in the Supporting Information (Figures S1-S3).

4.2. Membrane model

The stage cut (θ) for the membrane is defined as:

$$\theta = \frac{V_p}{V_f} \tag{4}$$

where V_p and V_f are the permeate and feed flow rates (Scm^3/s), respectively.

Eqn (5) is the component balance equation for component i. It gives 4 independent equations for the four components in the feed subject to the constraints given by Eqn (6).

$$y_{p_i} = \frac{\frac{p_f x_{f_i}}{1-\theta}}{\frac{V_p t}{P_i' A_m} + \frac{\theta p_f}{1-\theta} + p_p} \tag{5}$$

Table 2
Specifications of the rate-based model used for simulation.

Model Description	MEA	NH_3
Rate kinetics	Hikita et al. (1979)	Pinsent et al. (1956)
Mass transfer correlation	Bravo et al. (1985)	Onda et al. (1968)
Heat transfer correlation	Chilton and Colburn (Taylor and Krishna, 1993)	Chilton and Colburn (Taylor and Krishna, 1993)
Flow model	Mixed	Mixed
Liquid phase film resistance	Disrxn	Disrxn
Gas phase film resistance	No film	No film

Table 3
Numerical parameters for rate-based models.

Parameter	Description	Range	MEA	NH_3
NADP	Number of axial discretization points in the column	22–110	55	55
NFDP	Number of discretization points in the liquid film	2–10	5	5
FDR	Discretization ratio for the points in the liquid film	1.5–3	2.5	2.5
MCF	Averaging factor for calculating thermodynamic factors and transport resistances	0.25–0.75	0.25	0.5
RCF	Averaging factor for calculating reaction rates	0.25–0.75	0.75	0.5

$$s.t.\; y_{p_i} > 0 \; \forall i \; and \; \sum_{i=1}^{n} y_{p_i} = 1 \tag{6}$$

where V_f and x_f are the feed flow and composition, P_i' is the permeance of the ith component, p_f and p_p are the feed and permeate pressures ($cmHg$) respectively, and t and A_m are the thickness and area of the membrane.

Thus, for a chosen value of θ, Eqns (5) and (6) constitute a system of five coupled nonlinear algebraic equations with five unknowns, namely four component mole fractions on the permeate side (y_{p_i}) and the required membrane area (A_m). The remaining variables are the known process parameters and consitute the inputs. These may be solved using any available nonlinear equation solver. Alternately, the equations may be solved sequentially as a trial and error problem starting with calculation of A_m from Eqn (7) for a guessed value of y_{p_1}, which is then used to calculate the remaining y_{p_i} values from Eqn (5) and the process is repeated until the constraints are fulfilled. The latter was adopted in this study.

$$A_m = \frac{V_p y_{p_1} t}{P_1' \left[\frac{p_f \left(x_{f_1} - \theta y_{p_1} \right)}{1-\theta} - p_p y_{p_1} \right]} \tag{7}$$

5. Simulation results and cost estimation

In this section, process simulation results for the CCC technologies under study is presented. Additionally, discussions on cost of capture, OPEX/CAPEX breakdowns, and contributions from different sections of a given capture system are also included.

For cost estimation, the methodology of Turton et al. (2008) is followed. The capital expenditure ($CAPEX$) and operating expenditure ($OPEX$) for the CCC are calculated using Eqs. (8-11):

$$CAPEX = 1.18 \sum_{j \in E} CBM_j \times \frac{CEPCI_{currentyear}}{CEPCI_{baseyear}} \tag{8}$$

where E is the set of all equipment in the CCS process, CBM_j is the bare module cost of the jth equipment, and CEPCI is the Chemical Engineering Plant Cost Index. Detailed costing equations for bare module costs of different equipment are summarized in the supplementary information.

Annualized values of capital expenditure, and fixed and variable operational expenditure for a given rate of depreciation (r) and plant life (n) are estimated as follows:

$$CAPEX_a = \text{CAPEX} \times \frac{r(1+r)^n}{(1+r)^n - 1} \tag{9}$$

$$FOPEX_a = 0.1 CAPEX_a \tag{10}$$

$$VOPEX_a = CP \times \sum_{j \in CU} F_j + EP \times \sum_{j \in EU} P_j + \sum_{j \in RM} RP_j \times RM_j \quad (11)$$

where CP and EP are the set of equipment consuming cooling water and electricity respectively, F_j and P_j are the annual cooling water flow and power requirements for the jth equipment in the set, RM_j is the annual consumption of the jth raw material, and CP, EP, and RP_j are the prices of cooling water, electricity, and jth raw material.

The total annualized cost of capture per tonne of CO_2 ($/tCO$_2$) is given as follows:

$$TAC = \frac{CAPEX_a + FOPEX_a + VOPEX_a}{tCO_2} \quad (12)$$

where tCO_2 is the amount of CO_2 (tonnes) captured annually.

The values of $VOPEX_a$ and tCO_2 depend on the time spent by the vessel at sea in a year, which is assumed to be 8 months in this work. A depreciation of 8 % and plant life of 25 years is used, unless otherwise specified.

5.1. Absorption with MEA

The major CAPEX components for the separation section are the costs of absorber and regenerator columns. The absorber column height is decided by studying the variation in solvent flow rate with varying height for a fixed recovery of 90 %. It was fixed at 12 m, as beyond this height the solvent flow rate does not reduce significantly with increasing height, thus bringing diminishing returns for additional capital investment. The column diameter is calculated to ensure the operation is at 70 % of the flooding limit. The dimensions of the absorber and regenerator columns for both HFO and LNG run ships are summarized in Table 4. The process parameters and design performance of the capture setup are summarized in the Appendix (Table A1).

The cost contributions of the different units to the TAC for MEA-based capture is presented in Fig. 6. The TAC for LNG and HFO cases are estimated to be 82 $/tCO$_2$ and 127 $/tCO$_2$. For the case of HFO, the waste heat available from the exhaust gas does not completely fulfil the energy demand for regeneration with a deficit of 2.6 MW. This thermal energy deficit is assumed to be fulfilled by operating the existing ship reboiler at a higher load. The TAC for HFO results in a separation expense of 59 $/tCO$_2$ and an additional $6 t/CO$_2$ for the desulphurization unit . A lower separation cost of 41 $/tCO$_2$ is observed for a LNG powered vessel as it has a higher exhaust gas temperature thus eliminating the need for additional energy for regeneration. A lumpsump cost of ~6 $/tCO$_2$ was estimated for the drying unit (~100 % Moisture Removal) for both cases. Details of the drying unit will be communicated in a future work. The combined costs of compression and liquefaction of CO_2 for HFO and LNG fuels are 37 $/tCO$_2$ and 17 $/tCO$_2$. A lower estimated cost for LNG is due to the availability of the cold energy. This has the potential to reduce the cooling duty by ~90 %. Lastly, based on the effective CO_2 capture, BOG generation rate, voyage duration, and 85 % filling criteria, the storage volumes of CO_2 for the LNG and HFO case are calculated to be 686 m^3 and 1424 m^3 respectively and translate to a storage cost of ~18 $/tCO$_2$ for both cases. The OPEX contributions from various sections are shown in Fig. 7.

5.2. Absorption with NH_3

Similar to the MEA section, the primary CAPEX contributors are the columns for the CO_2 and NH_3 separation units. The column dimensions for both HFO and LNG (see Table 5) were calculated following the same method discussed in the previous section. Assessed from the column dimensions, the combined column footprint from CCC and abatement sections for both fuels is quite high compared to the MEA case. Similar to the CO_2 absorption section, the abatement section also includes heat exchange between the NH_3 rich and NH_3 lean streams (with a minimum approach temperature of 5 °C) to reduce the reboiler load. The model process parameters for the capture system is presented in the supporting information.

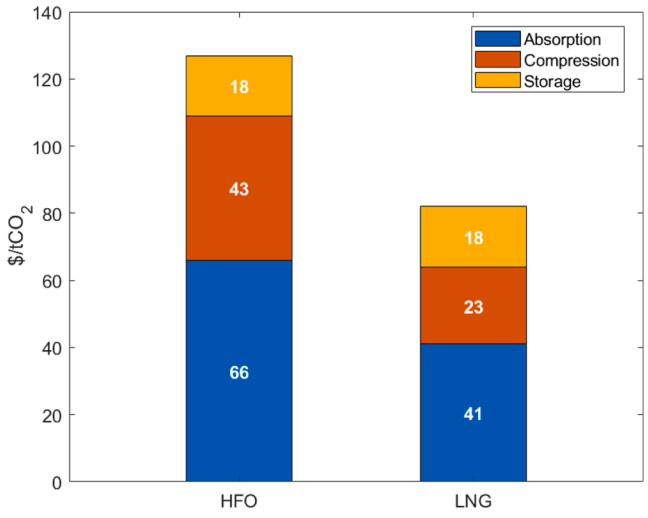

Fig. 6. Capture costs in the MEA based capture system for both fuel cases.

As described in Section 3.2, decreasing the solvent temperature results in a 40 % reduction in NH_3 slip, thereby requiring lesser wash flow in the abatement section leading to lesser reboiler duty. Despite the efforts to reduce the thermal load, the heat energy from the flue gas is insufficient to cater to the thermal demand of the system and can only fulfil 36 % and 45 % of the demand for HFO and LNG respectively. This is a result of the reboiler duty, stemming from NH_3 regeneration in the abatement section. However, one of the issues with operation at low temperatures is that beyond a certain lean loading for a given feed concentration, precipitation of NH_4HCO_3 is observed (Darde et al., 2009; Zhuang et al., 2011). In this study, this problem is circumvented by operating at a lean solvent loading below the point where precipitation starts to occur.

The TACs for the NH_3 process are estimated to be 260 $/tCO$_2$ and 231 $/tCO$_2$ for HFO and LNG fuels. They are significantly higher compared to the MEA process (reported in the previous section). The TAC for the HFO case is ~13 % higher than the LNG case for NH_3 process (see Fig. 8) as opposed to 55 % in the MEA process. This can be attributed to the fact that a major portion of the cost stems from the abatement section which is similar for both fuels since comparable amounts of NH_3 are processed both cases. Additionally, in the case of NH_3 solvent, the reboiler duties for the two fuels are not as different as that for the MEA solvent (see supplementary info). Further, the cost of the cryogenic process in the compression section is lower here because the regenerator operates at a higher pressure (6 bar).

Costs for compression and liquefaction are 29 $/tCO$_2$ and 9 $/tCO$_2$ for HFO and LNG cases respectively. Drying CO_2 incurs a cost comparable to the outlined in the MEA section. On an operational cost front, the major cost comes from the operation of the chillers, coolers and reboiler units. The contribution from operational cost of the CCC is 65 % and 76 % for LNG and HFO run ships respectively. The cost breakdown of the OPEX (Fig. 9) shows that the costs associated with the operation of CO_2 absorption section mainly stem from the cooling duty, whereas the reboiler duty is the major contributor to OPEX for the abatement section.

Table 4
Column dimensions for MEA based capture.

Fuel	Abs-D (m)	Abs-L (m)	Reg-D (m)	Reg-L (m)
HFO	3.36	12	1.35	4.05
LNG	2.82	12	0.95	2.85

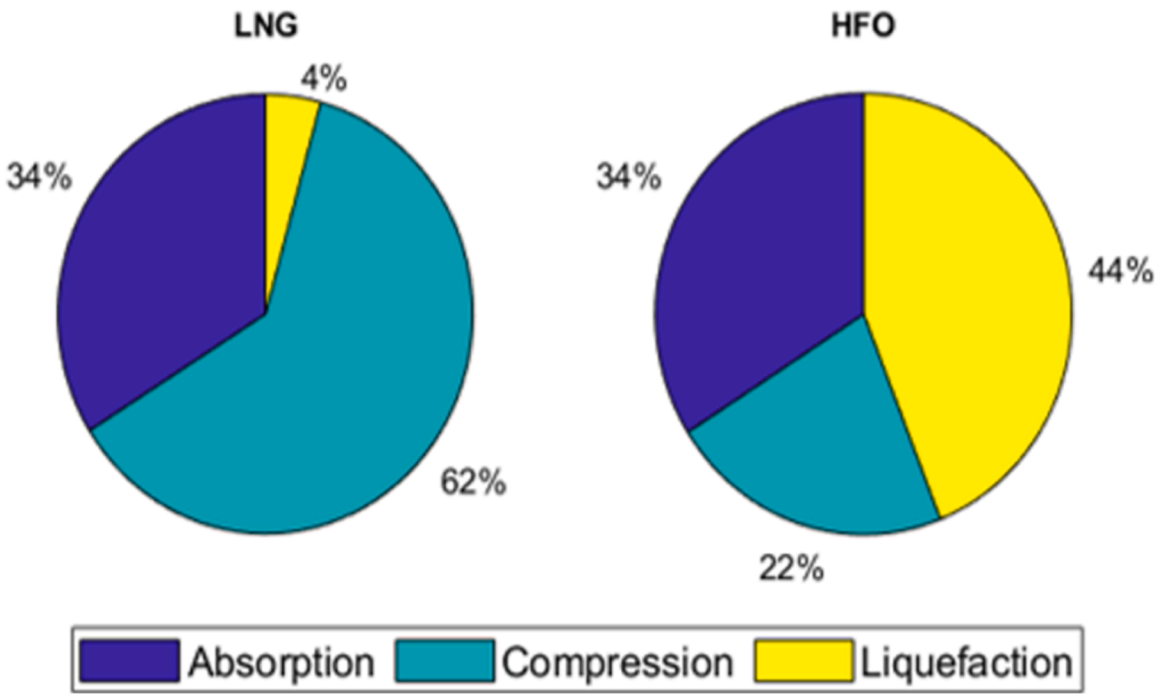

Fig. 7. OPEX distribution in the MEA based capture system for both fuel cases.

Table 5
Column dimensions for NH_3 based capture.

Fuel	CO_2 Abs-D (m)	CO_2 Abs-L (m)	CO_2 Reg-D (m)	CO_2 Reg-L (m)	NH_3 Abs-D (m)	NH_3 Abs-L (m)	NH_3 Reg-D (m)	NH_3 Reg-L (m)
HFO	5	24	1.65	4.95	4.5	13.5	2.5	7.5
LNG	4.5	24	1.35	4.05	4	12	2.35	7.05

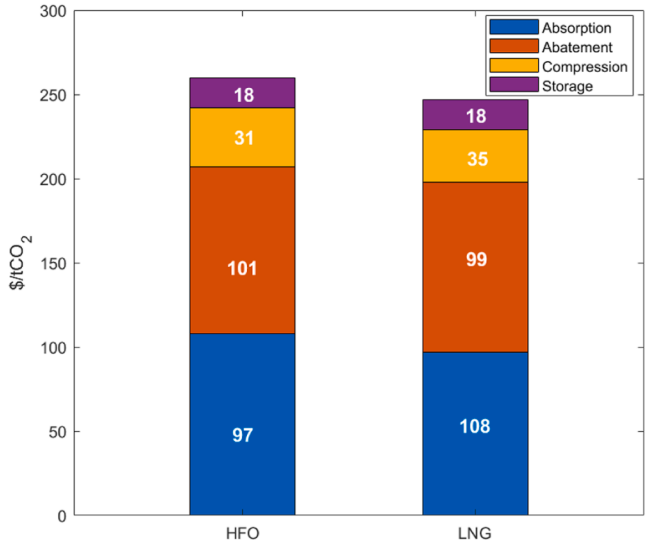

Fig. 8. Capture costs in the NH_3 based capture system for both fuel cases.

From an overall assessment stand point, the simulations provide evidence that even though NH_3 has the advantanges of a higher absorption capacity and non-corrosive nature, the associated costs for capture are much higher compared to the MEA process.

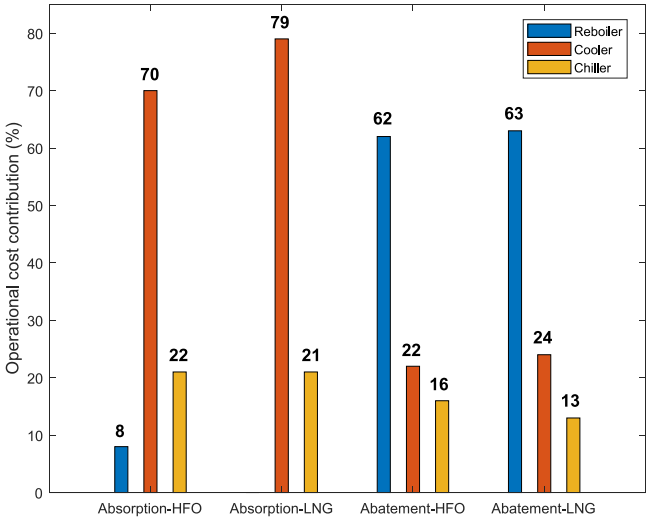

Fig. 9. OPEX distribution in the NH_3 based system for LNG and HFO fuel cases.

5.3. Cryogenic condensation

The TAC of cryogenic condensation was estimated to be 752 $/tCO$_2$ and 682 $/tCO$_2$ for HFO and LNG (excluding storage cost), with compression cost accounting for 52 % and 66 % respectively. The power required for compression in case of the HFO fuel is 6740 kW whereas for the LNG fuel it is 4800 kW. Cold energy integration reduces the cooling demand by 87.6 % (81 % from N_2 and 6 % from LNG) and 77 % for LNG and HFO respectively. Even though significant cold energy is available from the N_2 component of the exhaust gas for CO_2 condensation, the potential to reduce the liquefaction cost is still limited due to the factors such as low CO_2 concentration and high exhaust volumetric flow (~18 times and ~25 times compared to the CO_2 vapour flowrates from the MEA process regenerator top for HFO and LNG fuels respectively). Hence, a standalone cryogenic condensation unit at these flue gas conditions does not seem viable due to high compression and liquefaction

costs. However, the costs of compression and liquefaction can be reduced by increasing concentration of CO_2 in the feed. To this end, simulation studies are presented in the next section.

5.4. Effect of CO_2 concentration on cryogenic condensation cost

In this section, simulation studies are conducted to understand the effect of feed conditions on TAC. For simplification, the exhaust gas is assumed to be a binary mixture of N_2 and CO_2. The case studies are simulated for increasing CO_2 concentrations while maintaining same exhaust gas CO_2 flowrate in the feed (on increasing the CO_2 concentration, the feed flow reduces). The costs of the compression and liquefaction section are estimated by varying the concentration of CO_2 in the exhaust stream. Figs. 10 and 11 provide cost curves for the overall cost of carbon capture, compression cost and liquefaction cost for both cases.

It is observed that the overall cost reduces with increasing CO_2 concentration in the inlet flue gas due to a decrease in the total flowrate and the boiling point of the mixture approaching closer to that of CO_2. The reduction is more when LNG cold is available. However, since cold N_2 availability reduces with increasing CO_2 concentration, the cost advantage diminishes with increasing CO_2 concentration. Interestingly, in the case of LNG it is seen from Fig. 11 that liquefaction costs are lower than the compression costs below 40 wt % CO_2. This is the result of additional LNG cold that is available during liquefaction, which lowers the cooling and compression burdens in the liquefaction unit.

From the cost curves, we conclude that cryogenic condensation of CO_2 for HFO fuel is not economically viable for any raised CO_2 concentration in feed. In case of LNG, at CO_2 concentration of 80 wt % there stands a window of 6 \$/tCO_2 for addition of a pre-concentration unit with N_2 refrigerant as a competitor against MEA based absorption. On increasing CO_2 concentration to 95 wt %, the cost margin increases to 30 \$/tCO_2. Hence, for an LNG fuelled ship, an upstream process must enrich $CO_2 \geq 80$ wt % in the flue gas. We shall discuss the possibility of such an integration after discussing membrane-based separation in the next section.

5.5. Membrane separation

In this section, the possibility of using membrane separation technology for CCC is assessed. The membrane properties (Table 6) along with the CO_2/N_2 and O_2/N_2 selectivities are taken from Oh et al. (2022). CO_2/H_2O selectivity is assumed to be unity as suggested in the literature for high values of CO_2 permeance (Ramasubramanian et al., 2012). The

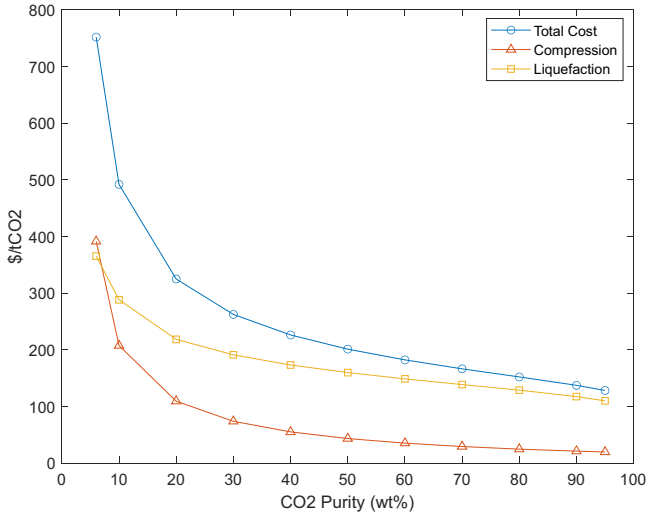

Fig. 10. TAC vs CO_2 concentration for cryogenic process with HFO as fuel.

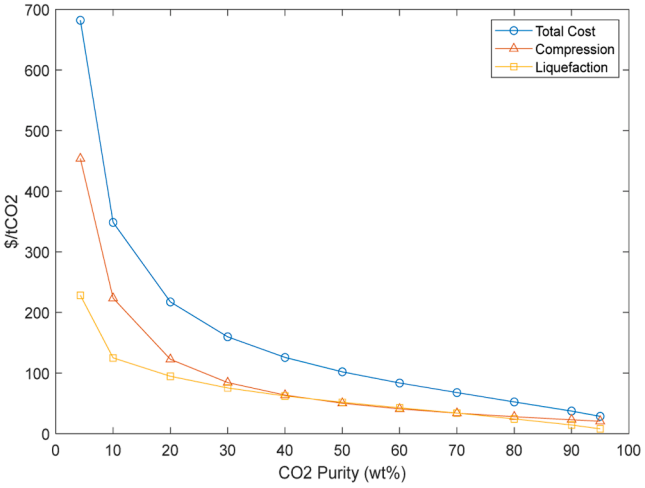

Fig. 11. TAC vs CO_2 concentration for cryogenic process with LNG as fuel.

Table 6
Membrane properties and operating parameters.

Property	Value
Thickness (cm)	10^{-5}
Area/module (m^2)	2500
Volume/module (m^3)	5
Vacuum pressure (bar)	0.05
CO_2 permeance (GPU)	1000
CO_2/N_2 selectivity	50
O_2/N_2 selectivity	5
CO_2/H_2O selectivity	1

simulations are carried out for CO_2 permeances of 1000 (base case), 2000, and 3000 GPU with permeances of N_2 and O_2 fixed at 20 and 100 GPU respectively. Due to the presence of moisture in the flue gas, it is imperative for the membrane system to operate at a temperature that is high enough to avoid condensation on either side of the membrane. The permeated water vapor is removed by cooling the second stage permeate to 45 °C before it is compressed and liquefied.

Through preliminary simulations for the flue gas from the LNG case, it is found that recycling is mandatory as even for a CO_2 permeance of 3000 GPU the maximum achievable purity for 90 % recovery without recycling is ~15 wt %. For recycling, the recycled retentate stream composition must be greater than the feed concentration so that the effective feed concentration rises. In our simulations, the viable set of stage cuts for 90 % recovery always leads to the first stage recycle as zero. This is because the retentate composition is always lower than the feed composition for the set of possible values of first stage cut (θ_1). Similarly, for a given θ_1, an upper bound is imposed on the second stage cut (θ_{2max}). Beyond this value, the retentate concentration falls below the feed concentration. Fig. 12 shows the variation of recovery and purity values with number of membrane modules for recoveries more than 80 %. These points correspond to a pre-specified θ_1 and its corresponding θ_{2max}. It is observed that the number of modules increases 2–3 times as the recovery increases beyound 80 %. It is also observed that for higher recoveries the difference between the number of modules required for different selectivities reduces. However, there are considerable differences between the purities.

The membrane cost and life were assumed to be 26.9 \$/m^2 and 4 years respectively (Ramasubramanian et al., 2012). For CO_2 permeance of 3000, and recovery and purity of 90 % and 62 wt % respectively, the cost (CAPEX+FOPEX) for membrane is calculated to be in excess of 500 \$/tCO_2. Even if the membrane costs get halved and its life time doubled, the cost of separation for membranes is over three times to that of MEA-based absorption. Similar estimates were obtained for HFO as well

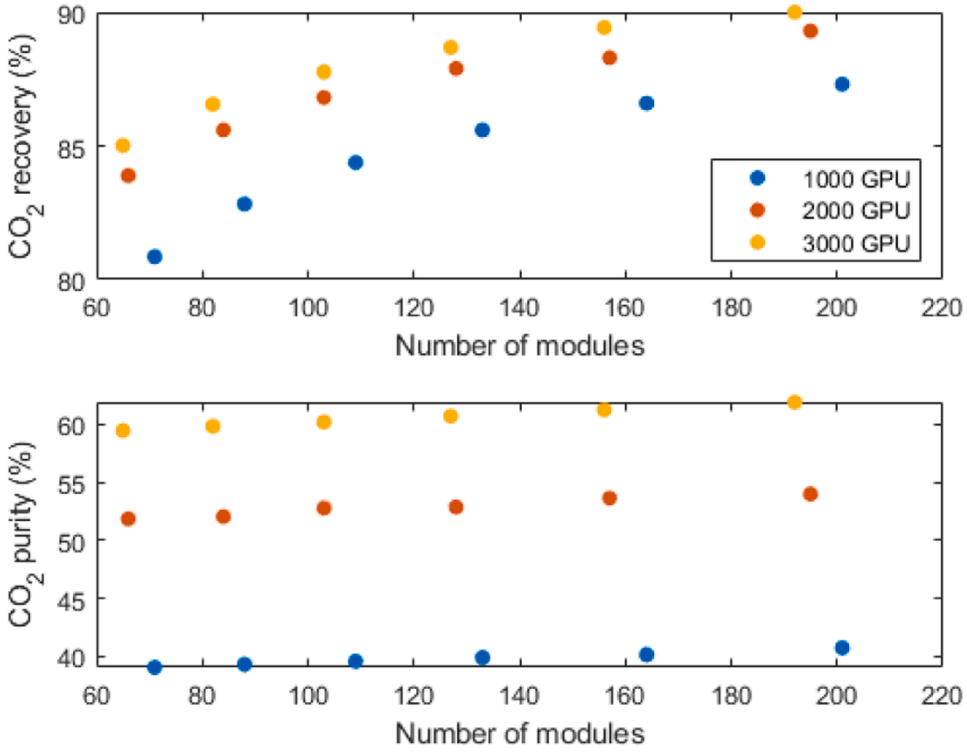

Fig. 12. Recovery and Purity variation with number of modules.

and have been omitted for the sake of brevity. It is apparent that even the most optimistic cost estimate far exceeds the minimum cost of the MEA-based absorption process. Hence, the possibility of synergistic hybrid process combining membrane and cryogenic processes, raised in the previous section seems infeasible at this time.

6. KPI summary for best technology

Simulation studies in the previous sections provide evidence that MEA-based absorption is the best technology for onboard capture in terms of the TAC of the processes compared. In this section, we provide the key KPIs (defined in Table A3) for the two fuel cases after CCC integration in a newly built MR Tanker (see Table 7).

The daily CO_2 capture for HFO is almost double compared to LNG (81 kg/h versus 41 kg/h) as the flue gas flowrate and the CO_2 concentration are both higher for HFO. Due to the higher flue gas and CO_2 flow rates, the CCC unit for HFO requires bigger equipment, thus contributing to a higher CAPEX. Hence, the additional CAPEX for the CCC w.rt. the cost of a newly built MR Tanker is higher for HFO than LNG (41 % versus 24 %). The energy penalty for CCC in the LNG case is insignificant compared to HFO case owing to the availability of higher heat energy stemming from the high flue gas temperature and the inherent LNG cold energy. Hence, the fuel penalty and extra CO_2 emissions are much higher for HFO, thus leading to an effective capture of merely 75 % as opposed to ~ 90 % for LNG.

Table 7
KPIs for CCC onboard an MR tanker.

KPI		LNG	HFO
CO_2 captured (tonnes/day)		41	81
Effective capture (%)		88	75
Energy Penalty (MJ/tCO2)		403	2278
Fuel Penalty (kg/h)		14 (1.8%)	198 (19%)
Extra CO_2 emitted (kg/h)		39	627
Additional CAPEX (%)		24	41
Cargo loss	Volume	None	None
	Weight (tonnes)	842 (1.8%)	1545 (3.3%)

Fig. 13 shows the fuel and liquid CO_2 storage tank (LCO_2) volumes as well as their locations on the ship. For a tanker, installation of CCC does not lead to any loss of cargo volume as there is no storage above the deck and hence the CCC equipment do not compete for space with the cargo. It is assumed that for safe operation of the ship, its Dead Weight Tonnage (DWT) has to be maintained. Hence, the additional weight from the CCC has to be compensated by reduction in cargo transported during the course of the voyage. The cargo losses in terms of weight for LNG and HFO are estimated to be 1.8 % and 3.3 % respectively - the captured LCO_2 is the most significant contributor for the cargo loss (73 % of 1.8 % for LNG and 83 % of 3.3 % for HFO).

7. Conclusion

Absorption with MEA and NH_3, cryogenic condensation, and membrane separation were assessed as potential technologies for CO_2 capture onboard a MR tanker for two fuels, LNG and HFO. The TAC was selected as the primary criteria with the constraints of 90 % and 95 % on the recovery and purity of CO_2. The MEA-based absorption process outperforms all other technologies by a fair margin with TACs of 76 $/t$CO_2$ and 121 $/t$CO_2$ for the LNG and HFO cases respectively. NH_3-based absorption fails to compete because of high costs of NH_3 abatement, whereas cost of compression makes the cost of cryogenic condensation prohibitive. To alleviate the compression cost, the possibility of a hybrid technology via a enrichment unit followed by cryogenic condensation is considered. It is found that the inclusion of an alternative pre-concentrator technology with cryogenics using N_2 refrigerant even when LNG cold is available does not hold weight for further investigation. Further, membrane separation was evaluated as a potential CCC technology; however, due to the high cost and short life of the membrane compared to other technologies, it is also ruled out.

For the best technology (MEA-based absorption), other KPIs like cargo losses, additional energy requirements, effective CO_2 capture, and additional CAPEX were also evaluated. From these KPIs, it can be concluded that CCC for LNG is better suited than HFO for the ship under

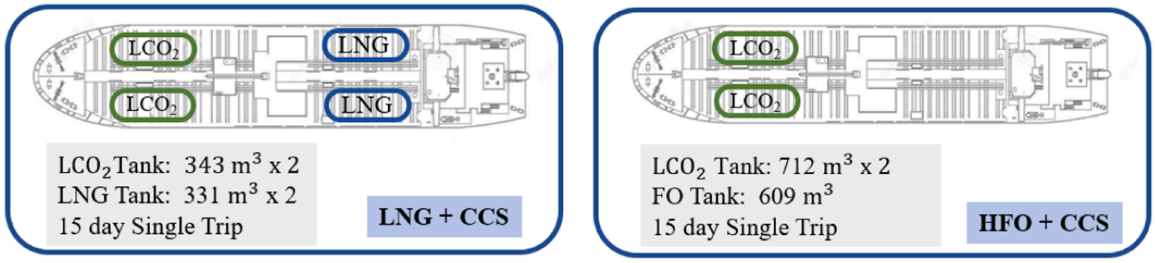

Fig. 13. Schematic and dimensions of fuel and LCO_2 tanks for the two cases.

study. In addition to lower TAC, it requires lower additional CAPEX, has higher effective recovery, and incurs lower cargo losses. Even if we were to incorporate costs of HFO and LNG in the evaluation, LNG will still be favoured, because the fuel costs are similar ($/kJ), and the energy demand for HFO run ships is much higher due to a lower exhaust temperature and absence of cold energy. Lastly, to the best of our knowledge, there are no firmly specified and widely accepted cost targets for CO_2 capture in the maritime industry. However, for CCC to be economically feasible, the cost of capture for the best technology should not exceed the carbon tax.

To build on the findings from the present study, we are evaluating the efficacy of the best technology (MEA-based absorption) for LNG run ships with different flue gas conditions, voyage durations, and number of trips. Avenues for optimal energy integration are also being explored. The findings will be reported in a future communication.

CRediT authorship contribution statement

Preethi Sridhar: Methodology, Software, Writing – original draft. **Anikesh Kumar:** Methodology, Software, Writing – original draft. **Sanjith Manivannan:** Methodology. **Shamsuzzaman Farooq:** Conceptualization, Writing – review & editing. **Iftekhar A. Karimi:** Conceptualization, Writing – review & editing.

Declaration of Competing Interest

The authors declare the following financial interests/personal relationships which may be considered as potential competing interests:

IA Karimi reports financial support was provided by Neptune Orient Lines Ltd.

Data availability

No data was used for the research described in the article.

Acknowledgements

This project was funded under the NOL fellowship (NOLF) grant award 2020. The NOL Fellowship is an initiative by Neptune Oriental Lines Ltd (now under the CMA CGM group) and NUS to develop first-rate research programme on transport and logistics issues.

Supplementary materials

Supplementary material associated with this article can be found, in the online version, at doi:10.1016/j.compchemeng.2023.108545.

Appendix

Tables A1, A2, A3

Table A1
Operating Parameters for CO_2 absorption with MEA solvent.

Process Unit	Variable	HFO	LNG
Desulphurization	$L/G\ (kg/kg)$	2	–
	SO_x *in exhaust gas* (ppm)	473	–
	SO_x *capture* (%)	99	–
CO_2 Absorber	$T_{exhaustgas}\ (^{\circ}C)$	45	45
	$T_{lean-solvent}\ (^{\circ}C)$	40	40
	$L/G\ (kg/kg)$	1.71	1.28
	$(mol\ CO_2/mol\ MEA)_{lean}$	0.30	0.30
	$Conc_{MEA}\ (wt\%)$	30	30
	$Conc_{CO_2}\ (wt\%)$	6.3	4.3
	Water makeup (kg/h)	979	1663
	MEA makeup (kg/h)	13.09	6.26
CO_2 Regenerator	$T_{rich-solvent}\ (^{\circ}C)$	106	107
	$(mol\ CO_2/mol\ MEA)_{rich}$	0.46	0.45
	Reboiler duty (MW)	4.07	2.10
	$P_{reg}(bar)$	2	2

Table A2
Operating Parameters for CO_2 absorption with NH_3 solvent.

Process Unit	Variable	HFO	LNG
Desulphurization	$L/G\ (kg/kg)$	2	–
	$SO_x\ in\ exhaust\ gas\ (ppm)$	473	–
	$SO_x\ capture\ (\%)$	99	–
CO_2 Absorber	$T_{exhaustgas}\ (^\circ C)$	45	45
	$T_{CO_2lean}\ (^\circ C)$	10	10
	$L/G\ (kg/kg)$	3.21	2.76
	$(mol\ CO_2/mol\ NH_3)_{lean}$	0.15	0.15
	$P_{abs}\ (bar)$	1	1
	$NH_3\ concentration\ (wt\%)$	10	10
	$CO_2\ concentration\ (wt\%)$	6.3	4.3
	$NH_3\ Slip\ (ppm_v)$	55,000	50,000
CO_2 Regenerator	$T_{CO_2rich}\ (^\circ C)$	105	105
	$(mol\ CO_2/mol\ NH_3)_{rich}$	0.35	0.35
	$Reboiler\ duty\ (MW)$	5.32	4.51
	$P_{reg}\ (bar)$	6	6
NH_3 Absorber	$L/G\ (kg/kg)$	2.4	2.1
	$T_{water}\ (^\circ C)$	15	15
	$P_{abs}\ (bar)$	1	1
NH_3 Regenerator	$T_{NH_3rich}\ (^\circ C)$	85	85
	$(mol\ CO_2/mol\ NH_3)_{lean}$	0.35	0.35
	$Reboiler\ duty\ (MW)$	9.51	7.32
	$P_{reg}(bar)$	1	1
	$NH_3\ regenerated\ (kg/s)$	1.10	0.91

Table A3
Definitions of KPIs used in Table 7.

KPI	Definitiom
CO_2 captured	It is defined as the tonnes of CO_2 captured by the CCC per day of a voyage.
Effective capture	It is defined as the percent of CO_2 captured by the CCC with respect to the total CO_2 emitted including emissions arising from the energy demands of the CCC.
Energy Penalty	It is defined as the extra energy required (MJ) by the CCC per tonne of CO_2 captured, in addition to the energy available from hot and cold integration.
Fuel Penalty	It is defined as the extra fuel burnt (kg/h) to cater to the energy penalty incurred by the CCC.
Extra CO_2 emitted	It is defined as the extra CO_2 emitted (kg/h) as a result of the fuel penalty.
Additional CAPEX	It is defined as the increment in CAPEX incurred by the installation of CCC with respect to the cost of a new built ship.
Cargo loss	It is defined as the percentage loss of cargo (volume/weight) incurred by the installation of CCC.

References

Adu, E., Zhang, Y.D., Liu, D., Tontiwachwuthikul, P., 2020. Parametric process design and economic analysis of post-combustion CO_2 capture and compression for coal- and natural gas-fired power plants. Energies 13.

Amirkhosrow, M., Pérez-Calvo, J.F., Gazzani, M., Mazzotti, M., Nemati Lay, E., 2021. Rigorous rate-based model for CO_2 capture via monoethanolamine-based solutions: effect of kinetic models, mass transfer, and holdup correlations on prediction accuracy. Sep. Sci. Technol. 56, 1491–1509.

Aspelund, A., Mølnvik, M.J., De Koeijer, G., 2006. Ship transport of CO_2: technical solutions and analysis of costs, energy utilization, exergy efficiency and CO_2 emissions. Chem. Eng. Res. Des. 84, 847–855.

Awoyomi, A., Patchigolla, K., Anthony, E.J., 2019. CO_2/SO_2 emission reduction in CO_2 shipping infrastructure. Int. J. Greenhouse Gas Control 88, 57–70.

Awoyomi, A., Patchigolla, K., Anthony, E.J., 2020. Process and economic evaluation of an onboard capture system for LNG-fueled CO_2 carriers. Ind. Eng. Chem. Res. 59, 6951–6960.

Bravo, J.e.L., Rocha, J.A., Fair, J.R., 1985. Mass transfer in gauze packings. Hydrocarbon Process. 64, 91–95.

Darde, V., Thomsen, K., van Well, W.J.M., Stenby, E.H., 2009. Chilled ammonia process for CO_2 capture. Energy Procedia 1, 1035–1042.

Eide-Haugmo, I., Brakstad, O.G., Hoff, K.A., da Silva, E.F., Svendsen, H.F., 2012. Marine biodegradability and ecotoxicity of solvents for CO_2-capture of natural gas. Int. J. Greenhouse Gas Control 9, 184–192.

Einbu, A., Pettersen, T., Morud, J., Tobiesen, A., Jayarathna, C.K., Skagestad, R., Nysæther, G., 2022. Energy assessments of onboard CO_2 capture from ship engines by MEA-based post combustion capture system with flue gas heat integration. Int. J. Greenhouse Gas Control 113, 103526.

Feenstra, M., Monteiro, J., van den Akker, J.T., Abu-Zahra, M.R.M., Gilling, E., Goetheer, E., 2019. Ship-based carbon capture onboard of diesel or LNG-fuelled ships. Int. J. Greenhouse Gas Control 85, 1–10.

Geankoplis, C.J., 2003. Transport Processes and Separation Process principles: Includes Unit Operations, 4th ed. Prentice Hall, Upper Saddle River, NJ. Professional Technical Reference.

Hikita, H., Asai, S., Katsu, Y., Ikuno, S., 1979. Absorption of carbon dioxide into aqueous monoethanolamine solutions. AIChE J. 25, 793–800.

IMO. (2015). Third IMO greenhouse gas study 2014. In. London.

IMO. (2021a). Cutting GHG Emissions from Shipping - 10 years of Mandatory Rules. In (Vol. 2023): IMO.

IMO. (2021b). Fourth Greenhouse Gas Study 2020. In Greenhouse Gas Study. London.

Jayaweera, I., Jayaweera, P., Yamasaki, Y., Elmore, R., 2016. 8 - Mixed salt solutions for CO_2 capture. In: Feron, P.H.M. (Ed.), Absorption-Based Post-combustion Capture of Carbon Dioxide. Woodhead Publishing, pp. 167–200.

Lewis, W.K., Whitman, W.G., 1924. Principles of gas absorption. Indus. Eng. Chem. 16, 1215–1220.

Liu, J., Gao, H.C., Peng, C.C., Wong, D.S.H., Jang, S.S., Shen, J.F., 2015. Aspen Plus rate-based modeling for reconciling laboratory scale and pilot scale CO_2 absorption using aqueous ammonia. Int. J. Greenhouse Gas Control 34, 117–128.

Luo, X., Wang, M., 2017. Study of solvent-based carbon capture for cargo ships through process modelling and simulation. Appl. Energy 195, 402–413.

Niu, Z., Guo, Y., Zeng, Q., Lin, W., 2012. Experimental studies and rate-based process simulations of CO_2 absorption with aqueous ammonia solutions. Ind. Eng. Chem. Res. 51, 5309–5319.

Notz, R., Mangalapally, H.P., Hasse, H., 2012. Post combustion CO2 capture by reactive absorption: pilot plant description and results of systematic studies with MEA. Int. J. Greenhouse Gas Control 6, 84–112.

Oh, J., Anantharaman, R., Zahid, U., Lee, P., Lim, Y., 2022. Process design of onboard membrane carbon capture and liquefaction systems for LNG-fueled ships. Sep. Purif. Technol. 282, 120052.

Onda, K., Takeuchi, H., Okumoto, Y., 1968. Mass transfer coefficients between gas and liquid phases in packed columns. J. Chem. Eng. Jpn. 1, 56–62.

Parry, I., Heine, D., Kizzier, K., Smith, T., 2018. Carbon Taxation for International Maritime Fuels: Assessing the Options. IMF.

Peh, S.B., Farooq, S., Zhao, D., 2023. Techno-economic analysis of MOF-based adsorption cycles for postcombustion CO_2 capture from wet flue gas. Chem. Eng. Sci. 268, 118390.

Pinsent, B.R.W., Pearson, L., Roughton, F.J.W., 1956. The kinetics of combination of carbon dioxide with ammonia. Trans. Faraday Soc. 52, 1594–1598.

Ramasubramanian, K., Verweij, H., Winston Ho, W.S., 2012. Membrane processes for carbon capture from coal-fired power plant flue gas: a modeling and cost study. J. Memb. Sci. 421-422, 299–310.
Ros, J.A., Skylogianni, E., Doedée, V., van den Akker, J.T., Vredeveldt, A.W., Linders, M. J.G., Goetheer, E.L.V., Monteiro, G.M.S., 2022. Advancements in ship-based carbon capture technology on board of LNG-fuelled ships. Int. J. Greenhouse Gas Control 114, 103575.
Shen, M., Tong, L., Yin, S., Liu, C., Wang, L., Feng, W., Ding, Y., 2022. Cryogenic technology progress for CO_2 capture under carbon neutrality goals: a review. Sep. Purif. Technol. 299, 121734.
SingaporeStatutesOnline. (2023). Environmental Protection and Management (Air Impurities) Regulations. In.
Song, C., Liu, Q., Deng, S., Li, H., Kitamura, Y., 2019. Cryogenic-based CO2 capture technologies: state-of-the-art developments and current challenges. Renewable Sustainable Energy Rev. 101, 265–278.
Stec, M., Tatarczuk, A., Iluk, T., Szul, M., 2021. Reducing the energy efficiency design index for ships through a post-combustion carbon capture process. Int. J. Greenhouse Gas Control 108, 103333.
Taylor, R., & Krishna, R. (1993). Multicomponent mass transfer. In.
Turton, R., Bailie, R., Whiting, Shaeiwitz, J, 2008. Analysis, Synthesis and Design of Chemical Processes. Pearson.
UNCTAD. (2020). Review of Maritime Transport 2020. In. New York.
Wärtsilä. (2019a). Super Trident sewage treatment plant - Large STC-14 series. In.
Wärtsilä. (2019b). Wärtsilä 46DF. In (Vol. 2023).
Yang, H., Xu, Z., Fan, M., Gupta, R., Slimane, R.B., Bland, A.E., Wright, I., 2008. Progress in carbon dioxide separation and capture: a review. J. Environ. Sci. 20, 14–27.
Yang, W., Li, S., Li, X., Liang, Y., Zhang, X., 2015. Analysis of a new liquefaction combined with desublimation system for CO_2 separation based on N_2/CO_2 phase equilibrium. Energies 8, 9495–9508.
Yeh, J.T., Resnik, K.P., Rygle, K., Pennline, H.W., 2005. Semi-batch absorption and regeneration studies for CO_2 capture by aqueous ammonia. Fuel Process. Technol. 86, 1533–1546.
Zhang, M., Guo, Y., 2013. Process simulations of NH3 abatement system for large-scale CO_2 capture using aqueous ammonia solution. Int. J. Greenhouse Gas Control 18, 114–127.
Zhuang, Q., Pomalis, R., Zheng, L., Clements, B., 2011. Ammonia-based carbon dioxide capture technology: issues and solutions. Energy Procedia 4, 1459–1470.